Journal of
Ceramic Science
and Technology

J. Ceram. Sci. Tech., 07 [04] 335-340 (2016)
DOI: 10.4416/JCST2016-00039
available online at: http://www.ceramic-science.com

Microstructure and Mechanical Properties of Ternary Ceramic Composites with a ZrC-SiC Matrix

B.X. Ma*, S.H. Xu

School of Materials Science and Engineering, Harbin University of Science and technology,
No. 4 Linyuan Road, Haerbin 150040, P. R. China

received May 16, 2016; received in revised form July 11, 2016; accepted August 29, 2016

Abstract

ZrC-SiC-$ZrSi_2$ ternary ceramic composites were prepared by means of hot pressing. The effect of the $ZrSi_2$ content on the microstructure and mechanical properties of the fabricated materials was investigated. It was found that the addition of $ZrSi_2$ is effective in promoting the sinterability of ZrC-SiC-$ZrSi_2$ ternary composites, and the highest relative density reaches 98.8 % when the $ZrSi_2$ content is 10 vol%. $ZrSi_2$ particles in the microstructure are characterized by an irregular shape with low dihedral angles, which is beneficial for the densification of the composites. The hardness of the composites shows no great variation with the increase in the $ZrSi_2$ content and changes between 14 and 17 GPa. The highest flexural strength, 520 MPa, is obtained for the composite of ZS5Z containing 5 vol% $ZrSi_2$.

Keywords: ZrC-SiC, $ZrSi_2$, microstructure, mechanical properties

I. Introduction

In the family of the ultra-high temperature ceramics (UHTCs), zirconium carbide (ZrC) possesses a high melting point (3420 °C) and hardness (25.5 GPa), excellent electrical conductivity and thermal conductivity, and it is available at a relatively low price [1–4], which makes it a candidate for thermal protection systems and propulsion components on future hypersonic flight vehicles and reusable launch vehicles [5,6].

Despite having the above excellent characteristics, the fracture toughness, sinterability and high-temperature oxidation resistance of single-phase ZrC ceramic are poor. An alternative approach for improving the properties of ZrC ceramic is the addition of secondary or ternary phase into the ZrC matrix, which can restrain grain growth, increase the relative density and improve the fracture toughness. Attempts at this have been made with several additives, such as $MoSi_2$ [7,8], SiC [9,10], ZrO_2 [11–13] and Mo [14,15]. Recent works have indicated that the incorporation of compounds containing silicon can obtain finer microstructure and better mechanical properties and higher oxidation resistance based on the formation of a silica or mixed oxide layer such as zircon ($ZrO_2 \cdot SiO_2$) [16–19]. Among these silicon-containing species, SiC is frequently selected as a reinforcing phase in composite materials. In previous works, the sinterability and fracture toughness were improved with the addition of SiC particles [9,10]. Other additives such as $ZrSi_2$ are emerging as effective for densification, which has been proved in ZrB_2-based ceramics [20,21]. At the same time, oxidation resistance was also improved owing to the formation of a silica-based protective scale at high temperature. Based on this case, the purpose of the work described in this paper was to add $ZrSi_2$ particles into a ZrC-SiC matrix to fabricate ZrC-SiC-$ZrSi_2$ ternary ceramic composites. The effect of the addition of $ZrSi_2$ on the microstructure and mechanical properties of the composites was investigated. It was expected that the addition of $ZrSi_2$ could provide excellent oxidation resistance for ZrC, in addition to obtaining better mechanical properties.

* Corresponding author: mabaoxia@126.com

II. Experimental

Commercially available ZrC powder (mean particle size 1.25 μm, purity > 98.0 %, Wing High High-Tech New Material Co., Ltd., Changsha, China), SiC powder (mean particle size 2.0 μm, purity ≥ 99 %, Weifang Kaihua Micropowder Co., Ltd., Shandong, China), $ZrSi_2$ powder (mean particle size ~ 38μm, purity > 99.5 %, Tute Advanced Material Co., Ltd., Kunming, China) were used as the raw materials. The SiC content in the design compositions was fixed to 20 vol%, and the varying $ZrSi_2$ contents were 3, 5, 10 vol%, respectively. The corresponding composites were labeled ZS3Z, ZS5Z and ZS10Z, respectively. The corresponding compositions of the composites are listed in Table 1. The powder mixtures were wet-milled at 200 rpm for 16 h in a polyethylene bottle using ZrO_2 balls and ethanol as milling media, and subsequently dried in a rotary evaporator at a temperature of 70 °C and at a rotation speed of 110 rpm to minimize segregation. The obtained powder mixtures were placed in a graphite die with its inner walls coated with BN slurry to avoid interaction between the specimens and the graphite die. Then, hot pressing was performed at 1900 °C for 60 min under a uniaxial load of 30 MPa in an argon atmosphere.

Table 1: The composition and relative density of ZrC-SiC-$ZrSi_2$ composites.

Samples	Composition (vol%)			Relative density (%)
	ZrC	SiC	$ZrSi_2$	
ZS3Z	77	20	3	97.5
ZS5Z	75	20	5	98.5
ZS10Z	70	20	10	98.8

The actual density of the composites was determined using the Archimedes technique with distilled water as the immersing medium. Flexural strength was measured in a three-point bending test on specimen bars with the dimensions with 3 mm × 4 mm × 36 mm using a span of 30 mm and a crosshead speed of 0.5 mm/min. Fracture toughness was evaluated with the single-edge notched beam (SENB) test using 22 mm × 4 mm × 2 mm bars on the same jig used for the flexural strength, with a span of 16 mm and a crosshead speed of 0.05 mm/min. At least five specimens were tested for each experimental condition. Hardness was measured by means of Vickers indentation with 1 kg as the applied load for 15 s on polished surfaces. The phase compositions of the composites were analysed with an x-ray diffractometer (XRD) (X'Pert PRO, PANalytical). The microstructure of the composites was analyzed by means of scanning electron microscopy (SEM) (Model FEI Sirion-200, Holland and Model CamScan MX2600, England) equipped with an energy-dispersive x-ray spectrometer (EDS). The fracture surfaces of the specimens were examined with SEM.

III. Results and Discussion

Fig. 1 shows XRD patterns of all the composites. It can be seen that the phase compositions of the composites consist of ZrC, SiC and $ZrSi_2$ phases. In addition to these three phases, additional phase diffraction peaks are not observed in the diffraction curve, indicating that no new phases are formed during sintering process.

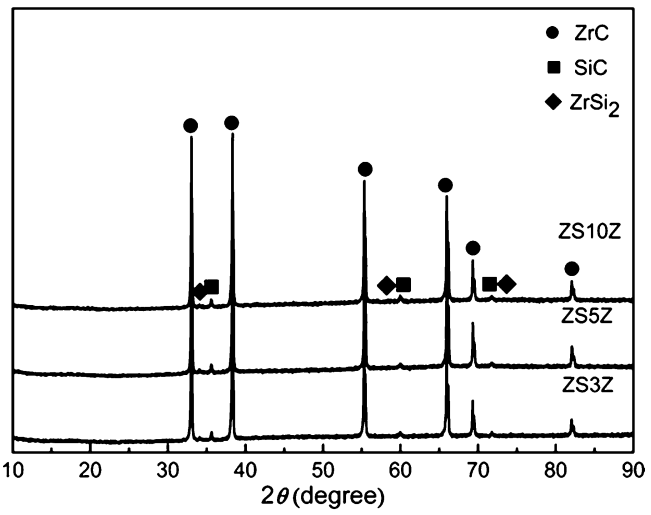

Fig. 1: XRD patterns of ZrC-SiC-$ZrSi_2$ composites with the different $ZrSi_2$ content.

The microstructures of ZrC-SiC-$ZrSi_2$ composites after polishing are shown in Fig. 2. It can be seen that the microstructures of the composites contain both gray phases and dark phases. The gray ZrC matrix is easily distinguishable; however, the dark SiC and $ZrSi_2$ phases are difficult to distinguish only by means of color. According to the characterization of raw materials, large numbers of small-sized dark phases are identified as SiC (~3 μm), and SiC particles are distributed uniformly in the ZrC matrix. $ZrSi_2$ particles have a broad size distribution. Some $ZrSi_2$ particles are fine, which is difficult to identify with SiC under secondary electron (SE) imaging. Microstructures of the composites were observed under backscattered electron (BSE) imaging. It can be seen from Fig. 3 that SiC and $ZrSi_2$ show no obvious contrast under backscattered electron (BSE) imaging, as expected. The light-gray phases are ZrC phases (bright contrast), and the phases with the darkest contrast are still SiC and $ZrSi_2$ mixed phases. BSE observation fails to identify these two phases. Some $ZrSi_2$ particles are very coarse, which is easy to observe (see the EDS pattern in Fig. 2(c)). Large $ZrSi_2$ particles are characterized by an irregular shape with low dihedral angles, as shown in Fig. 2(d). The characteristic morphology of $ZrSi_2$ is attributed to the ductile deformation behaviour of $ZrSi_2$ phase during hot pressing. The melting point of $ZrSi_2$ is ~ 1620 °C [20], and is lower than the sintering temperature of 1900 °C. Under the sintering temperature, the $ZrSi_2$ particles become ductile with the increase in temperature. This ductility can force $ZrSi_2$ particles to fill into the voids between the ceramic particles under the pressure during sintering, further improving the densification of the composites. This morphology change of $ZrSi_2$ particles is also observed in ZrB_2-based composites with $ZrSi_2$ [20,22].

In addition, obvious porosity is not observed in the microstructure. Table 1 is the relative density of the composites. The relative density is obtained according to the following rule. First, the theoretical densities of the composites were calculated according to the mixed law, assuming no impurities and no reactions during processing. Then the actual density was divided by the theoretical density to determine the relative density. It can be found that the relative density of ZrC-SiC-$ZrSi_2$ composites increases considerably with the increase in the $ZrSi_2$ content and the highest relative density reaches 98.8 % when the $ZrSi_2$ content is 10 vol%. It shows that a certain content of $ZrSi_2$ can effectively promote the sintering densification of ZrC composites. $ZrSi_2$ as a potential additive for lowering the sintering temperature was extensively introduced into boride-based ceramics, and the effect of the $ZrSi_2$ on the densification behavior was investigated. Previous studies conducted by Guo [20,23] revealed that the major cause for the improvement in densification was a formation of intergranular liquid phase between the $ZrSi_2$ and borides (ZrB_2, HfB_2, and TiB_2) owing to the interaction between the oxides (SiO_2 and B_2O_3) present on the surfaces of particles. For the ZrC-SiC-$ZrSi_2$ materials investigated in this study, XRD patterns of all the composites show that the phase compositions of the composites comprise ZrC, SiC and $ZrSi_2$ phases, whereas other phases such as ZrO_2 and SiO_2 are not found. Meanwhile, in the

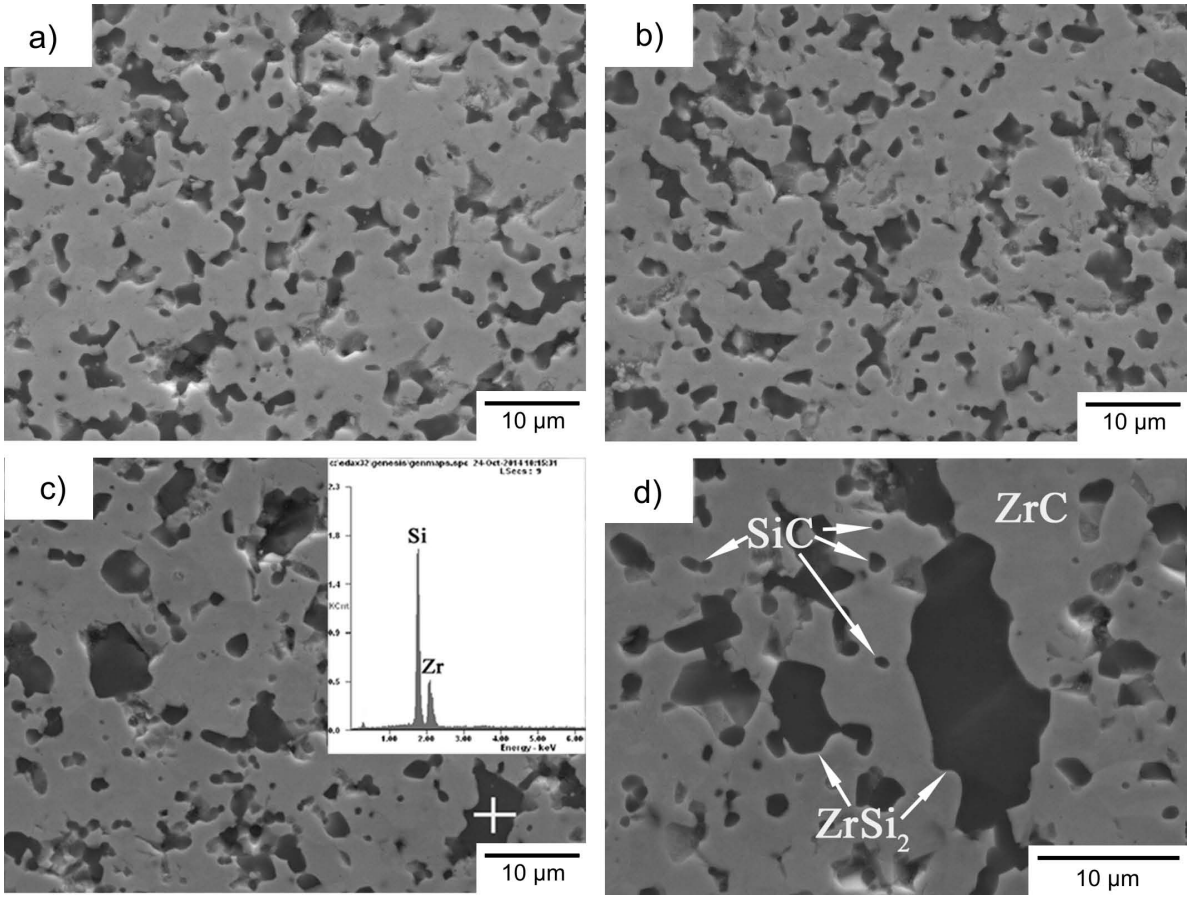

Fig. 2: SEM microstructures of polished surfaces of ZrC-SiC-$ZrSi_2$ composites with different $ZrSi_2$ content: (a) 3 vol%, (b) 5 vol%, (c) and (d) 10 vol%.

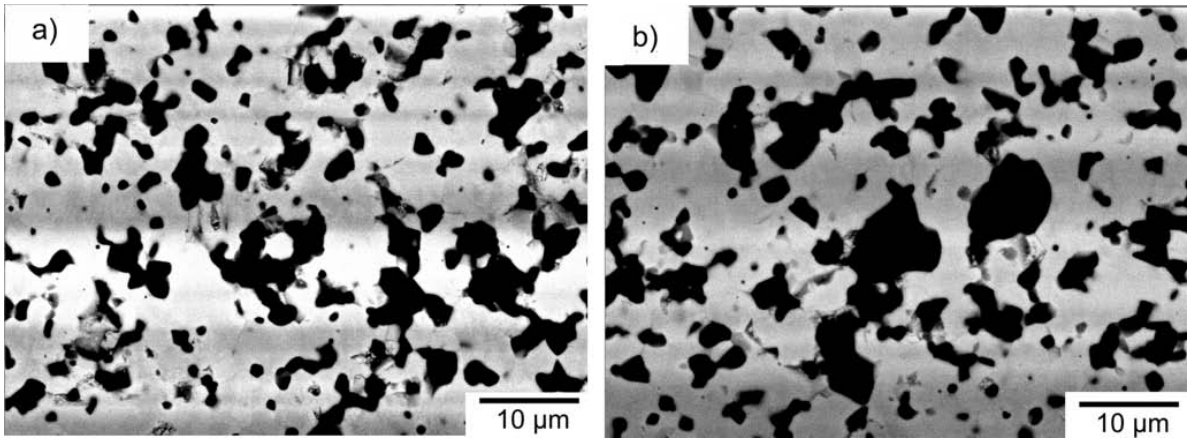

Fig. 3: Typical backscattered electron images of ZrC-SiC-$ZrSi_2$ composites: (a) 3 vol%, (b) 10 vol%.

microstructure of the composite, no liquid phase is traced, indicating that a similar densification mechanism does not appear for ZrC-based composites with $ZrSi_2$ in this study. Although the sintering temperature is higher than the $ZrSi_2$ melting point, $ZrSi_2$ does not seem to have a role as the liquid-phase sintering source. We believe that minor amounts of liquid phase may be present around initial $ZrSi_2$ particles at 1900 °C for 1 h. Longer holding times yields more liquid phase. However, owing to short holding time and subsequent cooling, such a liquid will quickly solidify, and liquid characteristics are hardly observable. Certainly, further research needs to be done.

The mechanical properties of ZrC-SiC-$ZrSi_2$ composites are listed in Table 2. The hardness of the composites shows no great variation with the increase in the $ZrSi_2$ content and changes between 14 and 17 GPa. The hardness is mainly influenced by the relative density of the composites and $ZrSi_2$ particles. The greater the relative density is, the higher the hardness is. However, the hardness value of the composites does not exhibit a similar change trend to the relative density. The main reason for this may be associated with low hardness of $ZrSi_2$ (10.63 GPa) [21]. The more $ZrSi_2$ is added, the more the hardness of the composites decreases. Therefore, the combination of both factors could be responsible for the change in the hardness trend.

Table 2: The mechanical properties of ZrC-SiC-$ZrSi_2$ composites.

Samples	Vickers Hardness (GPa)	Flexural Strength (MPa)	Fracture toughness ($MPa{\cdot}m^{1/2}$)
ZS3Z	15.13±0.17	505.10±0.66	3.42±0.04
ZS5Z	16.82±0.13	520.92±7.75	3.59±0.07
ZS10Z	14.33±0.14	403.11±3.57	2.81±0.09

In Table 2, the flexural strength of the composites increases with the increase in the $ZrSi_2$ content. The highest flexural strength, 520 MPa, is obtained for the composite of ZS5Z with 5 vol% $ZrSi_2$. When the content of the $ZrSi_2$ addition increases to 10 vol%, the flexural strength decreases significantly instead, even lower than that of ZrC-SiC composites, 448 MPa[24]. One explanation for the higher flexural strength of the ZS5Z with 5 vol% $ZrSi_2$ is its higher relative density owing to the proper addition of $ZrSi_2$. The decrease in the flexural strength for ZS10Z with 10 vol% $ZrSi_2$ is attributed to the presence of larger $ZrSi_2$ particles owing to the addition of a high volume fraction of $ZrSi_2$ in the composite. Therefore, excess $ZrSi_2$ in the composites is detrimental to the flexural strength.

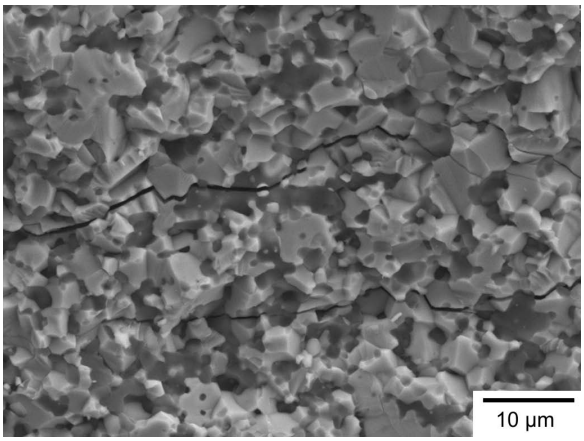

Fig. 4: SEM micrograph of microcracking on fracture surface of ZrC-SiC-$ZrSi_2$ composites.

For the fracture toughness of the composites, when the $ZrSi_2$ content is lower than 5 vol%, their values are comparable to 3.8 $MPa.m^{1/2}$ of ZrC-SiC composites [24]. The fracture toughness decreases drastically when the $ZrSi_2$ content increases to 10 vol%. From the microcracking of the fracture surface, as shown in Fig. 4, it is evident that the presence of $ZrSi_2$ does not obviously change the direction of the crack propagation such as crack deflection and crack branching, because a more tortuous crack path is instrumental to more energy consumption of crack propagation and a reduction of the crack driving force, further improving fracture toughness [12, 25]. In this present work, when the crack extends to $ZrSi_2$ particles, some $ZrSi_2$ particles crack, i.e. the crack is across the $ZrSi_2$ particles. The occurrence of the fracture of $ZrSi_2$ particles during crack propagation leads to no obvious contribution to the enhancement of the fracture toughness of the composites.

Fig. 5 shows the fracture morphology of ZrC-SiC-$ZrSi_2$ composites with different $ZrSi_2$ content. It can be seen that the fracture mode is a combination of intergranular fracture and transgranular fracture, where a transgranular fracture with a few ripple patterns is observed in the ZrC matrix, and where some ZrC grains generate the intergranular fracture. Furthermore, it is evident that SiC and $ZrSi_2$ particles are mainly distributed intercrystalline, and pull-out of SiC particles from the matrix can be observed, leaving a pit on the fracture surface.

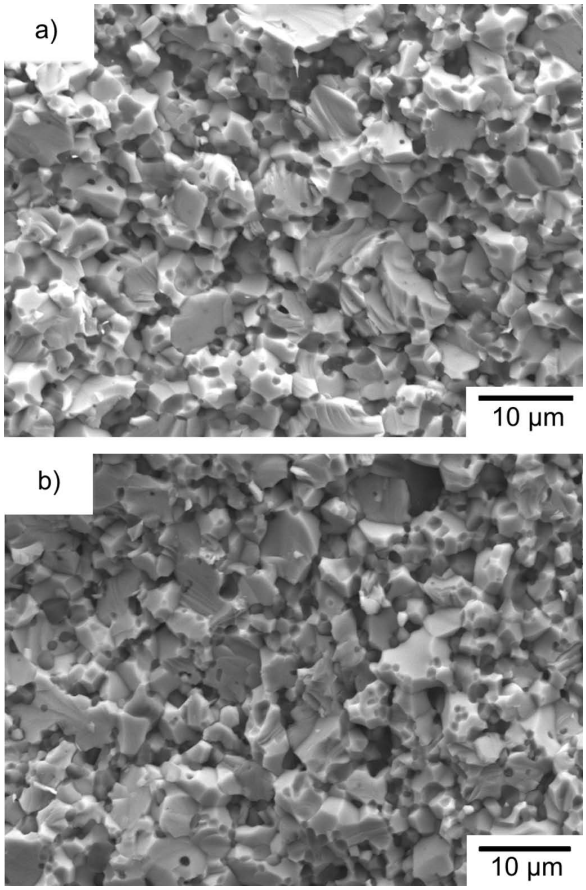

Fig. 5: Fracture morphology of ZrC-SiC-$ZrSi_2$ composites with different $ZrSi_2$ content: (a) 3 vol%, (b) 10 vol%.

IV. Conclusions

ZrC-SiC-$ZrSi_2$ ternary ceramic composites with high relative density can be prepared by means of hot-press-sintering at 1900 °C under 30 MPa for 60 min in a flowing argon atmosphere. The relative density of the composites containing 10 vol% $ZrSi_2$ reaches 98.8 %. The addition of $ZrSi_2$ has little influence on the hardness, ranging between 14 and 17 GPa. The flexural strength of the composites can be improved with the proper addition of $ZrSi_2$ particles, and the maximum flexural strength reached 520 MPa at 5 vol% $ZrSi_2$ content. Although the fracture toughness of the composites decreases drastically when the $ZrSi_2$ content is increased to 10 vol%, their values are comparable to the 3.8 $MPa.m^{1/2}$ of ZrC-SiC composites when the $ZrSi_2$ content is lower than 5 vol%. The fracture mode of the composites is a combination of intergranular fracture and transgranular fracture.

References

1. Goutier, F., Trolliard, G., Valette, S., Maître, A., Estournes, C.: Role of impurities on the spark plasma sintering of ZrC_x-ZrB_2 composites, *J. Eur. Ceram. Soc.*, **28**, 671 – 678, (2008).
2. Das, B.P., Panneerselvam, M., Rao, K.J.: A novel microwave route for the preparation of ZrC-SiC composites, *J. Solid. State. Chem.*, **173**, 196 – 202, (2003).
3. Bandyopadhyay, T.K., Das, K.: Processing and characterization of ZrC-reinforced steel-based composites, *J. Mater. Process. Tech.*, **178**, 335 – 341, (2006).
4. Patra, N., Jayaseelan, D.D., Lee, W.E.: Synthesis of biopolymer-derived zirconium carbide powder by facile one-pot reaction, *J. Am. Ceram. Soc.*, **98**, 71 – 77, (2014).
5. Opeka, M.M., Talmy, I.G., Zaykoski, J.A.: Oxidation-based materials selection for 2000°C + hypersonic aero surfaces: theoretical considerations and historical experience, *J. Mater. Sci.*, **39**, 5887 – 5904, (2004).
6. Jackson, T.A., Eklund, D.R., Fink, A.J.: High speed propulsion: performance advantage of advanced materials, *J. Mater. Sci.*, **39**, 5905 – 5913, (2004).
7. Sciti, D., Guicciardi, S. Nygren, M.: Spark plasma sintering and mechanical behaviour of ZrC-based composites, *Scripta Mater.*, **59**, 638 – 641, (2008).
8. Núñez-González, B., Ortiz, A.L., Guiberteau, F., Padture, N.P.: Effect of $MoSi_2$ content on the lubricated sliding-wear resistance of ZrC-$MoSi_2$ composites, *J. Eur. Ceram. Soc.*, **31**, 877 – 882, (2011).
9. Lucas, R., Davis, C.E., Clegg, W.J., Pizon, D., Babonneau, F., Foucaud, S., Antou, G., Maître, A.: Elaboration of ZrC-SiC composites by spark plasma sintering using polymer-derived ceramics, *Ceram. Int.*, **40**, 15703 – 15709, (2014).
10. Zhao, L.Y., Jia, D.C., Duan, X.M., Yang, Z.H., Zhou, Y.: Low temperature sintering of ZrC-SiC composite, *J. Alloy. Compd.*, **509**, 9816 – 9820, (2011).
11. Voltsihhin, N., Hussainova, I., Kübarsepp, J., Traksmaa, R.: Processing and mechanical properties of ZrC-ZrO_2 composites, *Key. Eng. Mater.*, **604**, 258 – 261, (2014).
12. Hussainova, I., Voltšihhin, N., Cura, E., Hannula, S.P.: Densification and characterization of spark plasma sintered ZrC-ZrO_2 composites, *Mat. Sci. Eng. A.*, **597**, 75 – 81, (2014).
13. Min-Haga, E., Scott, W.D.: Sintering and mechanical properties of ZrC-ZrO_2 composites, *J. Mater. Sci.*, **23**, 2865 – 2870, (1988).
14. Landwehr, S.E., Hilmas, G.E., Fahrenholtz, W.G., Talmy, I.G., Wang, H.: Thermal properties and thermal shock resistance of liquid phase sintered ZrC-mo cermets, *Mater. Chem. Phys.*, **115**, 690 – 695, (2009).
15. Landwehr, S.E., Hilmas, G.E., Fahrenholtz, W.G., Talmy, I.G., DiPietro, S.G.: Microstructure and mechanical characterization of ZrC-Mo cermets produced by hot isostatic pressing, *Mat. Sci. Eng. A..*, **497**, 79 – 86, (2008).
16. Zhao, L.Y., Jia, D.C., Duan, X.M., Yang, Z.H., Zhou, Y.: Oxidation of ZrC-30 vol% SiC composite in air from low to ultrahigh temperature, *J. Eur. Ceram. Soc.*, **32**, 947 – 954, (2012).
17. Sarin, P., Driemeyer, P.E., Haggerty, R.P., Kim, D.K., Bell, J.L., Apostolov, Z.D., Kriven, W.M.: *In situ* studies of oxidation of ZrB_2 and ZrB_2 -SiC composites at high temperatures, *J. Eur. Ceram. Soc.*, **30**, 2375 – 2386, (2010).
18. Wu, H.T., Zhang, W.G.: Fabrication and properties of ZrB_2-SiC-BN machinable ceramics, *J. Eur. Ceram. Soc.*, **30**, 1035 – 1042, (2010).
19. Wang, X.G., Zhang, G.J., Xue, J.X. Tang, Y., Huang, X., Xu, C.M., Wang, P.L.: Reactive hot pressing of ZrC-SiC ceramics at low temperature, *J. Am. Ceram. Soc.*, **96**, 32 – 36, (2013).
20. Guo, S.Q., Kagawa, Y., Nishimura, T.: Mechanical behavior of two-step hot-pressed ZrB_2-based composites with $ZrSi_2$, *J. Eur. Ceram. Soc.*, **29**, 787 – 794, (2009).
21. Wang, M.F., Wang, C.A., Zhang, X.H.: Effects of SiC platelet and $ZrSi_2$ additive on sintering and mechanical properties of ZrB_2-based ceramics by hot-pressing, *Mater. Design.,* **34**, 293 – 297, (2012).
22. Guo, S.Q., Nishimura, T., Kagawa, Y.: Low-temperature hot pressing of ZrB_2-based ceramics with $ZrSi_2$ additives, *Int. J. Appl. Ceram. Tec.*, **8**, 1425 – 1435, (2011).
23. Guo, S.Q., Kagawa, Y., Nishimura, T., Tanaka, H.: Pressureless sintering and physical properties of ZrB_2-based composites with $ZrSi_2$, additive, *Scripta Mater.*, **58**, 579 – 582, (2008).
24. Ma, B.X., Zhang, X.H., Han, J.C., Han, W.B.: Microstructure and mechanical properties of ZrC-SiC-C_g ceramic prepared by hot pressing, *Rare Metal. Mat. Eng., 38, 890* – 893, (2009).
25. Sonber, J.K., Murthy, T.S.R.C., Subramanian, C., Krishnamurthy, N., Hubli, R.C., Suri, A.K.: Effect of $CrSi_2$ and HfB_2 addition on densification and properties of ZrB_2, *Int. J. Refract. Met. H.*, **31**, 125 – 131, (2012).